Charge state of C_{10} and C_5 energetic cluster ions in amorphous carbon targets: simulations

2006 J. Phys.: Condens. Matter 18 11357

(http://iopscience.iop.org/0953-8984/18/49/026)

INSTITUTE OF PHYSICS PUBLISHING JOURNAL OF PHYSICS: CONDENSED MATTER

J. Phys.: Condens. Matter **18** (2006) 11357–11370 doi:10.1088/0953-8984/18/49/026

Charge state of C_{10} and C_5 energetic cluster ions in amorphous carbon targets: simulations

E Nardi[1] **and T A Tombrello**[2]

[1] Department of Particle Physics, Weizmann Institute of Science, Rehovot 76100, Israel
[2] Basic and Applied Physics, California Institute of Technology, Pasadena, CA, USA

E-mail: eran.nardi@weizmann.ac.il

Received 23 August 2006, in final form 2 November 2006
Published 23 November 2006
Online at stacks.iop.org/JPhysCM/18/11357

Abstract

We present here detailed simulations of the interaction of energetic C_{10} and C_5 clusters at the energies of 1, 2, and 4 MeV per carbon atom with an amorphous carbon target. The spatial evolution of the cluster components is simulated accounting for both scattering and Coulomb explosion. The former is calculated by means of the Monte Carlo method while the latter is computed by means of molecular dynamics. The charge state of the individual cluster components is calculated as a function of penetration depth, and is determined by the competition between electron ionization and recombination. The results of calculations of the effect of the neighbouring cluster components on the suppression of the values of the charge state are presented and compared to the experimental values of Brunelle *et al*. Charge state suppression calculations for the 2 MeV/C clusters for both C_{10} and C_5 agree well with the experimental results for penetration depths of less than about 500 and 250 Å respectively, assuming the intracluster Coulomb potential is screened by four target valence electrons. At 4 MeV/C the results are similar although less screening is required; a possible explanation is the inability of the plasma to completely screen the higher velocity projectiles. The 1 MeV/C calculated results however differ in their behaviour from the 2 and 4 MeV/C cases.

(Some figures in this article are in colour only in the electronic version)

1. Introduction

The interaction of energetic carbon clusters with solids has recently been a topic of much experimental and theoretical activity. Two very recent papers dealing with the detailed simulation of various aspects of energetic cluster target interactions have been published [1, 2]. Experimental advances over the past several years have made it possible to accelerate large size carbon clusters to high energies and to study the wealth of effects connected with the

interaction of these clusters with solid targets. These phenomena include energy loss, track formation, secondary particle emissions, sputtering and a reduction in the charge state of the exiting fragments [3]. Upon entering the target, the binding electrons of the cluster are stripped away and ionization of each of the energetic cluster components proceeds as the cluster travels through the target. The ionization of the energetic cluster components is similar but not identical to the case of the interaction of individual energetic ions with solid targets. This is the topic which will be treated at length below. The motion of each of the individual cluster constituents within the target is determined by binary multiple scattering with the target nuclei as well as by their Coulomb repulsion with the other charged cluster components. Thus, as the cluster advances within the target the mutual separation between the cluster constituents increases. The focus of the present paper is on the average charge state of the energetic cluster components passing through thin foils as compared to that of the individually accelerated projectiles of the same kinetic energy. Electron capture and electron loss by the energetic cluster components is modified by the presence of the other cluster constituents, such that the average charge state of the cluster components is significantly lower (charge suppression) than that of the individual ionic projectile.

The present work addresses by means of simulation the recent experimental work of Brunelle *et al* [3] on the charge state of energetic C_{10} and C_5 clusters at the energies of 2 MeV per carbon atom, as well as at 4 and 1 MeV/C, interacting with an amorphous carbon target. The simulations described here are based on those of [1], which dealt with C_{60}, but no comparison to experimental charge suppression data was made there. The major difference between the present simulations and those of [1] is that in the former the effect of the intra-cluster Coulomb interaction was taken into account only for the ionization cross section. In the present paper this effect on the recombination cross section was included as well and was calculated using the Bohr and Lindhard [4] classical theory. In [2], comparison with the above mentioned experimental data of Brunelle *et al* [3] was made. However, only modifications of electron recombination due to the cluster environment were carried out using an empirical model, while the effect of the neighbouring cluster components on the bound electron ionization was not included.

Specifically, we investigate here the decrease in the mean average charge state of the cluster components (charge suppression) in comparison to the charge state of an independently and isolated fast ion of the same energy. The charge state suppression is calculated for five different cluster size, total cluster kinetic energy combinations, which well represent the experimental data of Brunelle *et al* [3]. The calculations are also performed as a function of thickness of the amorphous carbon target, and detailed comparisons to experimental results of Brunelle *et al* [3] are made. The intra-cluster Coulomb interaction between the cluster ions is detrimental to the process of charge state suppression [1, 2]. In particular, the charge state suppression is critically dependent on the amount of screening of this interaction, which in turn depends on the effective number of screening electrons, as discussed below. The variation of this quantity with cluster size and energy as well as with the penetration depth is presented and discussed.

Previous other work on the calculations of the charge suppression measured in [3] was carried out by Heredia-Avalos *et al* [5] as well as by Kaneko [6]. These authors calculated charge suppression only for the 2 MeV/C clusters, but did not report results for the 4 and 1 MeV/C clusters. Both these papers neglected multiple scattering of the cluster constituents as they penetrate the target, which as will be seen is the more important mechanism for cluster breakup. In addition, screening which is detrimental in the charge suppression calculation was not included in the intra-cluster Coulomb interaction in [6]. Wei *et al* [7] calculated the breakup of energetic C_{20} clusters in solids. These authors calculated the charge states of the individual cluster components, as well as the energy loss. The calculations made use of the

dielectric response formalism in order to calculate the dynamically screened potential between the cluster components; however, comparison to experimental data as in the case of [5, 6] could not be made.

In section 2 the basic theory and calculational procedures are described. In section 3 the results are presented, while in section 4 we discuss our conclusions.

2. Theory and calculations

2.1. Scattering and Coulomb repulsion

As in [1] the trajectories of the individual atoms comprising the cluster are calculated independently from the moment the cluster enters the solid. At this point it is assumed that no binding energy exists between the atoms constituting the cluster, thus also disregarding the possible effects of collective cluster states. The cluster constituents upon penetrating the target are scattered by the target atoms and repelled by the other cluster ionic components as a result of their mutual Coulomb interaction.

Scattering of each of the cluster components by the target atoms was treated independently. The simulations were carried out and described in [1], using the binary collision model of Moller *et al* [8], which was devised for amorphous targets. This procedure was used for clusters by Zaijfman *et al* [9] as well as more recently by Barriga-Carrasco and Garcia-Molina [10].

As in [1], Coulomb explosion is treated by means of molecular dynamics using the leapfrog algorithm. The forces driving the Coulomb explosion are derived from the screened two-body Coulomb potential, V_C [9],

$$V_C = (q_i q_j / r) \exp(-r/a) \tag{1}$$

where q_i and q_j are the charges of ions i and j, r the distance between them. The dynamic screening length a is assumed to be given by $a = v/\omega_p$, with v the projectile velocity and ω_p the plasma frequency of the valence electron gas, which is proportional to the number of valence or 'screening electrons'. Dynamic screening as well as the number of screening electrons per atom will be discussed below.

In the molecular dynamics simulation, the equations of motion of the system consisting here of the ten or five carbon ions are integrated using forces calculated as the sum over pairwise interactions, as given by the two body potential in equation (1). A detailed account of the numerics as well as the time steps involved in the calculation was described in [1]. The contribution of the wake forces to the expansion of the clusters was studied by incorporating this force into the calculation using the formulae given by Gemmell *et al* [11]. Results of calculations indicate that the weak forces have a negligible effect on the angular spread of the cluster constituents, thus they were neglected here.

2.2. Charge state calculation: ionization and recombination

The charge state of each of the cluster components was calculated for each individual ion as a function of penetration depth. The basic assumption of the model is that the energetic cluster upon entering and penetrating the target behaves like a system of independent energetic carbon atoms. Thus, the binding electrons of the cluster are assumed to be immediately stripped away [3]. Binding electrons on tight multifragment orbitals could be of importance, however, when treating other phenomena, such as cluster surface interactions. The charge state calculations are based here on the detailed computation of the bound electron capture cross section and of the bound electron loss cross sections of each of the carbon cluster constituents. We note here that the projectile charge states were calculated in [5–7] by different methods.

Loss of the projectile bound electrons is due to ionization resulting from the Coulomb interaction of these electrons with the nuclei of the target atoms. The model used here is the binary encounter approximation (BEA) [12]. The cross section for the ionization of a projectile electron in shell n, bound by energy U_n, is given by

$$\sigma_{\mathrm{I}} = (\pi \mathrm{e}^4 Z_{\mathrm{t}}^2 / U_n^2) G(V) \tag{2}$$

where $G(V)$ is a function of V, the scaled projectile velocity v/v_n, where v is the projectile velocity and v_n the orbital velocity of the bound electron. $G(V)$ was calculated by McGuire and Richard [13] and is based on detailed classical binary collision scattering calculations by Gryzinski [14]. Z_{t} denotes the effective charge of the screened target atoms for projectile ionization. We have adopted here the value of $Z_{\mathrm{t}} = 2.05$ from Schiwietz *et al* [15], which is based on the Thomas–Fermi model.

The classical model of Bohr and Lindhard [4] was used to calculate the recombination cross sections. This model, which was used very recently [16], involves a two stage calculation. First, we calculate the release distance, R_{r}, defined as the distance between ion and target electron, up to which the force exerted by the projectile on the electron in a given electron shell is greater than the binding force within the atom, F_{a}. Thus, where q is the projectile charge,

$$qe^2/R_{\mathrm{r}} = F_{\mathrm{a}}. \tag{3}$$

The second step deals with the question of whether the liberated electron is captured by the projectile, depending on whether the potential energy of binding in the projectile system is greater than the kinetic energy of the electron in this system. Bohr and Lindhard [4] assume that the strong ionic fields induced by the projectile during capture greatly reduce the bound electron velocity with respect to the atom. Consequently, they assume that the bound electron velocity v_{e} can be neglected. Thus according to them, where v is the projectile velocity,

$$qe^2/R_{\mathrm{c}} = 1/2mv^2. \tag{4}$$

For $R_{\mathrm{c}} > R_{\mathrm{r}}$ the capture cross section is simply $\sigma_{\mathrm{CAP}} = \pi R_{\mathrm{r}}^2$. Bohr and Lindhard also allow for capture if $R_{\mathrm{c}} < R_{\mathrm{r}}$. Denoting the Bohr radius within the atom of the bound electron by r_n, they stipulate, that since release is a gradual process, which takes place with a probability per unit time of the order of v_{e}/r_n and the time during which capture can occur is approximately R_{c}/v, the probability that the released electron will be captured is roughly $(v_{\mathrm{e}}/r_n)(R_{\mathrm{c}}/v)$. Thus for $R_{\mathrm{c}} < R_{\mathrm{r}}$ they approximate the capture cross section by

$$\sigma_{\mathrm{CAP}} = \pi R_{\mathrm{c}}^2 (v_{\mathrm{e}} R_{\mathrm{c}} / r_n v). \tag{5}$$

Bound electron recombination cross sections for the carbon ions C^{2+} and C^{3+} at the energy of 2 MeV, obtained using the classical Bohr–Lindhard [4] model, were compared to cross sections derived from the OBK model [17], with the scaling factor α as given in [18]. In the former case the classical cross section was 1.2 times higher than the corrected OBK, while in the latter case this factor was 1.7. Considering that the differences between calculated and experimental results can be greater than a factor of two [19], and this, for the simple cases of bare projectiles, the agreement between the classical and OBK results is satisfactory.

From the above discussion it follows that an empirical scaling factor is needed to calibrate the recombination cross section in order to obtain agreement with the experimentally determined charge state, since the BEA ionization cross sections also do not give the correct absolute results. The equilibrium charge state was determined experimentally by Stoller *et al* [20] and by Brunelle *et al* [3] for 2 MeV carbon ions, who obtained a charge state of 2.85 at the exit of the foil. In a very recent paper Lifshitz and Arista [21] summarize that the average charge of the ion inside the solid is well approximated by the charge state of the ion exiting the solid, also basing their argument on experimental evidence. The scaling factor needed in

the Bohr Lindhard theory for multiplying the recombination cross section is 1.30, provided the ionization cross section is that calculated by the BEA model, equation (2). Dependence of the results on the absolute values of the cross sections is discussed below.

2.3. Charge state suppression and dynamical screening

Charge state suppression is due to the influence of the neighbouring cluster components on the ionization and recombination cross sections of each of the individual cluster components. Following reference [2] and as in [1], the additional ionization energy needed to remove each bound electron from the proximity of its ion and away from the cluster, ΔI_i, is given by

$$\Delta I_i = \sum_{j(\neq i)} q_j \left(\frac{\mathrm{e}^{-r_{ij}/a}}{r_{ij}} \right) \tag{6}$$

where r_{ij} is the distance between the jth ion and ion i, and a is the dynamical screening length discussed above and given by $a = v/\omega_\mathrm{p}$, where v is the projectile velocity and ω_p the plasma frequency given by $(4\pi Ne^2/m_\mathrm{e})^{1/2}$; e and m are the electron charge and mass, respectively. Dynamical screening, which is a most critical issue in these calculations and which is not taken into account in [6], is discussed in detail in the next paragraph. The critical quantity which determines a is N, the density of the effective number of valence or screening electrons, the determination of which is a non-trivial issue, as will be discussed below. Using equation (6) we obtain an increase in the ionization potential of the projectile electrons, which decreases with increasing cluster penetration and breakup. By thus increasing the binding energy of the projectile electron and in accordance with the BEA model used here, equation (2), the ionization cross section decreases, thus inducing a reduction in the projectile charge state. The increase in the projectile binding energy as given in equation (6) affects as well the recombination process by making it easier for the electron to recombine. Adding ΔI to the left-hand side of equation (4) brings about an increase in R_c, thus making the recombination cross section larger, thereby adding to charge state suppression. The cluster constituents can also increase the force on the bound target electron (see equation (3)), thus influencing the release distance R_r. This effect was studied for the cluster treated in this paper and found to be negligible.

The dynamically screened Coulomb potential is crucial in the charge suppression calculations through equation (6) (it also appears in equation (1)). This potential has been extensively used in the literature. It has been derived by Brandt [22], Lindhard [23], Nagy and Bergara [24] and very recently by Lifshitz and Arista [25] based on the extended Friedel sum rule. The latter authors stress the fact that this is an approximation, in particular the assumption of spherical symmetry. In deriving the screening length, a, they assumed a spherical potential of the form given in equation (1), deriving the value of a on the basis of the extended Friedel sum rule. The actual screening is much more complex; Jakubassa [26] compared the screening of an ion moving through a free electron gas to the simple form given by the exponent in equation (1). Analysis of the hydrogen ground state in the full dynamically screened potential was carried out by this author [26], who obtained fairly good agreement with the spherically symmetric potential based on the dynamic screening relation given above. Good agreement of the eigenvalues was obtained for the calculated values using the two types of screening. It could be argued that simple exponential screening could be a sufficiently good approximation at relatively small distances from the moving ion, failing at distances larger than several atomic radii, as will be addressed here when analysing the results.

Dynamical screening of the projectile Coulomb field in amorphous carbon was observed experimentally by Chevallier *et al* [27]. These authors observed a velocity threshold for the

binding of the 3p state of fast He^+ ions inside the target. As the velocity becomes larger the screening length increases as well, bringing about an effective decrease in screening. Thus for velocities higher than a threshold velocity, the 3p level, initially unbound at the lower velocities, becomes bound, as was found experimentally. The screening length for the solid amorphous target is computed using $a = v/\omega_p$, with relatively good agreement with experiment.

3. Results

3.1. Cluster breakup

The results presented in this paper on charge state suppression are for the C_5 and C_{10} energetic clusters at the different kinetic energies quoted in the experiments of [3]. Data on cluster breakup and expansion are given in [3], with additional data from the same experiments also given in [2]. Some results of our simulations on the breakup of the cluster will be given here. These afford a comparison between our simulation results and the experimental data, as well as with the simulations of [2]. It is also our purpose to comment on the relative importance of scattering compared to Coulomb explosion.

The initial shape of the C_{10} cluster was assumed to be annular, since 90% of the clusters are of this shape [28], while the bond length between the carbon atoms in the isolated cluster was 1.3 Å; see [2]. The initial direction of motion of the cluster is along the z axis. The plane consisting of the annulus was chosen by random rotation perpendicular to the z axis. The shape of C_5 is assumed to be linear [28], and the initial directions of cluster motion were randomly orientated in space.

Cluster breakup and expansion was studied for the 2 MeV per atom C_{10} cluster, with emphasis on the relative importance of scattering compared to Coulomb explosion. Comparisons to the experimental results of [3] quoted in [2] and with the simulations of [2] were made for 40 and 5.3 μg cm^{-2} thick targets. The angular distribution of an isolated carbon ion was calculated for the 40 μg cm^{-2} target and the FWHM was found to be 10 mrad, in agreement with Hartman *et al* [2]. For the same target, the effect of the intracluster Coulomb interaction on the angular distribution was calculated and compared to the experiment. This was done by calculating the angular distribution of an isolated carbon projectile and comparing to the angular distribution obtained for the cluster ions. The Coulomb interaction within the cluster in our calculations was screened by four valence electrons, which as seen below fitted well to the experimental charge suppression data. The angular distribution is broadened by less than 5%, employing the screened Coulomb repulsion. The experimental results presented in [2] indicate that within the experimental error of $\pm 5\%$ no difference exists between the angular distribution of a single isolated ion and the C_{10} cluster. For the thinner target of 5.3 μg cm^{-2} (230 Å) the experiment gives a ratio of 1.3 ± 0.1 for the ratio of the widths of the angular distribution of the C_{10} cluster to the isolated carbon ion. Our calculated ratio using the same assumption as above regarding Coulomb screening is 1.2, within the experimental error. However, we did not account for the additional non-screened repulsion of each ion with the other cluster ions, after exiting the target. This could explain the somewhat lower width obtained in our calculation.

In the above context it is of interest to cite figure 6 of [2], which gives experimental data on lateral distribution of the cluster constituents compared to the individual carbon ion at the energy of 2 MeV/C. The width of the angular distribution of the cluster constituents approaches that of the individual carbon ions as the thickness of the foil increases. But, even for the thinnest foils, for example the 96 Å foil, the effect of scattering on the lateral spot size is more than 50%. The effect of the Coulomb explosion is even relatively less important at the point where the

cluster exits the target, since the measurements include the additional non-screened repulsion after the cluster exits the target. Scattering becomes even relatively more important for the 1 MeV/C cases.

The conclusion here is that scattering is a dominant factor in cluster breakup even for the thinnest foils employed in the experiments analysed here. Thus in order to study charge suppression, which is intimately associated with cluster breakup through equation (6), it is imperative to include scattering. We recall that scattering was not included in the calculations of [5] and [6], which both dealt with the charge suppression problem treated here.

3.2. Charge state results

Brunelle *et al* [3] have provided a wealth of experimental data concerning the decrease in the charge state of the individual cluster constituents of energetic small carbon clusters compared to the case of an isolated carbon ion (charge suppression). The clusters ranged from C_3 to C_{10} while the cluster kinetic energies took on values of 1, 2, and 4 MeV per carbon atom. Charge suppression was measured for the various cluster size, kinetic energy combinations at different exiting thicknesses up to 40 μg cm^{-2}. In this paper we represent this data by five different cluster size, kinetic energy combinations: C_{10} at 2 MeV/C and at 1 MeV/C (no experimental data exists for 4 MeV/C for C_{10}), and C_5 at 1, 2 and 4 MeV/C.

The charge state of the expanding cluster constituents was calculated as described above in detail up to the foil thickness of 40 μg cm^{-2} (1739 Å) for the 2 and 4 MeV/C clusters and up to 800 A for the 1 MeV/A clusters. The calculated results are presented with different assumptions regarding the number of electrons which screen the intracluster Coulomb potential, see equation (6). Specifically, results are given for four, one and zero screening electrons. Although it might seem non-physical to assume a number of screening electrons different from four, this issue is non-trivial. As is well known in plasma physics, for very high velocity projectiles relative to the plasma electron velocities, the plasma does not have time to 'see' the 'test charge', and thus does not have time to respond and shield [29], as it would for a low velocity projectile; this effect is also mentioned generally in [2]. For velocities which are not much larger than the plasma electron velocities, it is reasonable that the plasma only partially shields the projectile charge. This effect could in principle be calculated using the procedures outlined in [29]. Also, by presenting the results with zero screening electrons, the effect of the screening by the four valence electrons versus no screening can be clearly seen.

In figure 1 is plotted the average charge state of the C_{10} cluster components as a function of penetration depth, for the 2 MeV per carbon cluster up to the depth of 2000 Å. The cluster fragments are restricted according to the above description to carry integral values of charge, while entering the solid with the charge state value of zero. The results to be presented in figures 1–5 are these integer values averaged over the total number of cluster constituents. The spread in the number of significant charge states exiting the target is generally three charge state units. The calculated charge states presented for each of the screening assumptions are the result of averaging over 500 different cluster penetration simulations. The charge state of the individual independently moving carbon ion as a function of penetration depth is also presented in the graph. The small continuous decrease of the charge state is due to the slowly decreasing kinetic energy of the ion resulting from the stopping power of the medium. This effect is clearly manifested in the exiting kinetic energies as measured by Brunelle *et al* [3]. We note that in calculating the energy loss of the carbon ions as they penetrate the target no account of collective cluster effects on stopping was included, as seems to be the case from the experimental data of Brunelle *et al* [3]. The experimental points of Brunelle *et al* [3] for the different foil thicknesses are also plotted together with their error bars in figure 1 for the cluster.

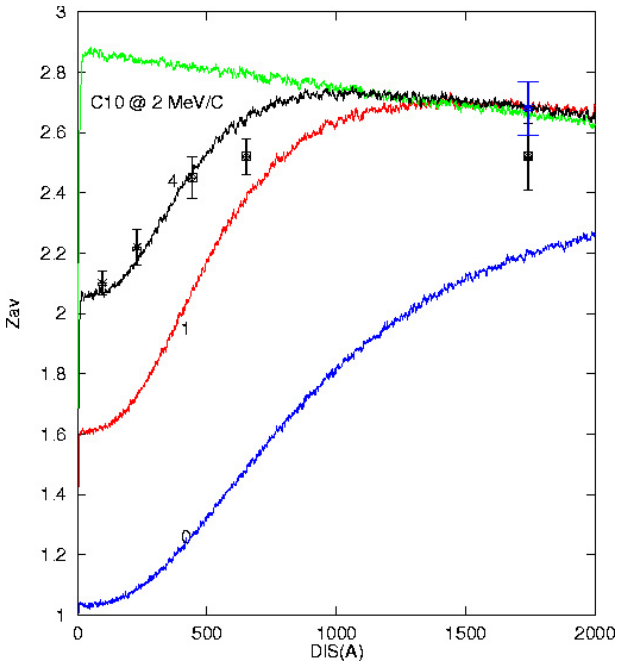

Figure 1. Average charge state of C_{10} clusters at 2 MeV/C as a function of penetration depth, in ångströms, in an amorphous carbon target averaged over 500 different random sequences. Plotted separately are the calculated average charge states for the Coulomb interaction screened by four, one and no target valence electrons, with the number of screening electrons denoted adjacent to the appropriate plot. The experimental results [3] are presented at five penetration depths. Also plotted is the calculated charge state for an individual carbon atom, which is the top curve. The experimental point at the largest experimental penetration depth for the latter case is drawn with the wide error bars.

In addition the measured charge state of the independently moving ion at 40 μg cm^{-2} is also plotted in the figures.

The striking feature in figure 1 is the good agreement between the calculated and experimental charge state for the first three points, up to the penetration distance of 443 Å, where four screening electrons are assumed in the calculation. However with increasing penetration, according to the model presented here, fewer screening electrons are needed to fit the experimental data. In particular at 1739 Å (40 μg cm^{-2}) between one and no electrons are required to fit the charge suppression which still exists at this point, as can be seen from the experimental points presented in the figure. The reason for this behaviour could be attributed to the far reaching simplifications in the screening model, which assumes symmetric screening using the approximate form of equation (1); this point will be discussed below. Thus, it would not be physically meaningful to attribute the values of zero or unity to the number of screening electrons for the thicker foils presented in figure 1.

The calculated results for C_5 at 2 MeV/C are plotted in figure 2 in a similar manner to that in figure 1. The results of the theoretical model in comparison to the experimental data fit the data essentially as well up to 230 Å (no experimental point at 443 Å) as in figure 1 for C_{10}, where the comparison was outlined above. It is interesting to note that the amount of charge suppression is clearly smaller for the C_5 cluster compared to C_{10}, due to the smaller number of cluster constituents.

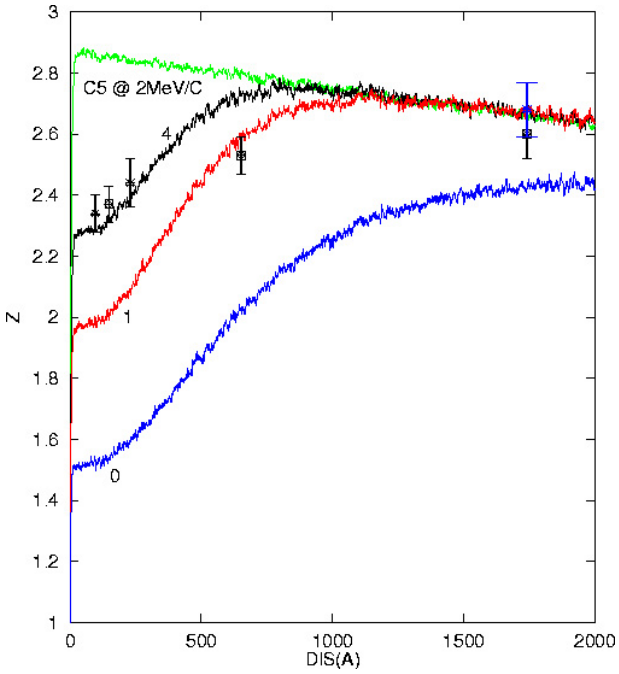

Figure 2. Average charge state of C_5 cluster at 2 MeV/C as a function of penetration depth, in ångströms, in an amorphous carbon target averaged over 500 different random sequences. Plotted separately are the calculated average charge states for the Coulomb interaction screened by four, one and no target valence electrons, with the number of screening electrons denoted adjacent to the appropriate plot. The experimental results [3] are presented at five penetration depths. Also plotted is the calculated charge state for an individual carbon atom, which is the top curve. The experimental point at the largest experimental penetration depth for the latter case is drawn with the wide error bars.

Brunelle *et al* [3] have also measured charge suppression data at the higher energy of 4 MeV/C only for C_5. Figure 3 is plotted in a manner similar to figures 1 and 2, where the experimental data are compared to our model with different assumptions regarding the number of screening electrons. The results of our model in comparison to experiment show the same trend as in figures 1 and 2; however, in the high energy case of figure 3, less screening, of the order of two screening electrons, is needed to fit the experimental data. This could be attributed, as mentioned above, to the situation where the plasma does not have enough time to respond and completely shield this faster projectile as compared to the slower moving 2 MeV/C ions. A point worth mentioning is the persistence in the calculation of the charge suppression at deeper penetration depths in comparison to the 2 MeV/C results of figures 1 and 2. This is a result of the slower breakup and expansion of the cluster resulting mainly from the smaller scattering as the energy increases.

Reference [3] also offers experimental charge suppression data at the lower energy of 1 MeV/C for the C_5 and C_{10} clusters, although for the former cluster up to 652 Å and for the latter only for 96 and 230 Å. In figure 4 we plot the C_5 experimental cluster data along with the results of our calculations, at 1 MeV/C, in a manner similar to the presentations in figures 1–3. The results of the present model for the C_5 cluster at 443 and 652 Å have roughly the same behaviour as the 2 MeV/C C_{10} case. However, the experimental point at 230 Å is significantly higher than the predicted charge suppression based on four screening electrons.

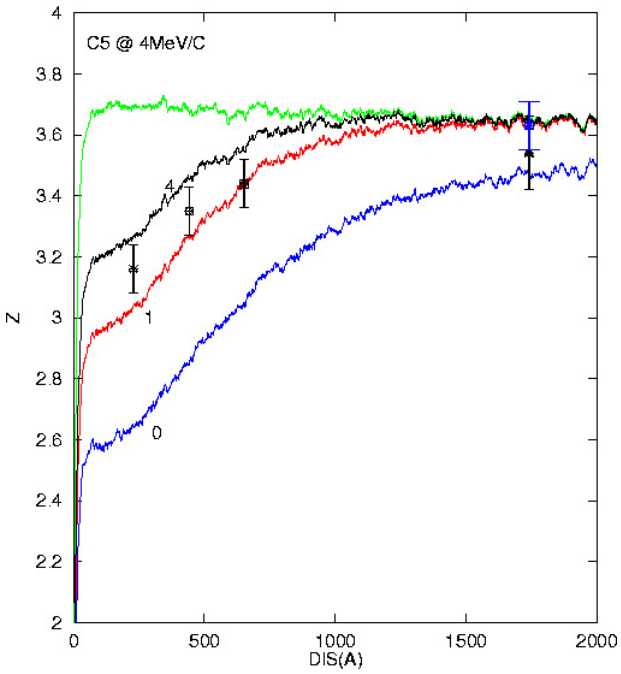

Figure 3. Average charge state of C_5 cluster at 4 MeV/C as a function of penetration depth, in ångströms, in an amorphous carbon target averaged over 500 different random sequences. Plotted separately are the calculated average charge states for the Coulomb interaction screened by four, one and no target valence electrons, with the number of screening electrons denoted adjacent to the appropriate plot. The experimental results [3] are presented at five penetration depths. Also plotted is the calculated charge state for an individual carbon atom, which is the top curve. The experimental point at the largest experimental penetration depth for the latter case is drawn with the wide error bars.

For the C_5 cluster at the lower energy of 2 MeV/C the experimental point at this depth is somewhat higher than the calculation but is still within the error bar of the experimental result.

In figure 5 we present in a manner similar to the other figures the results for the C_{10} cluster at the lower energy of 1 MeV/C. The two experimental points at 230 and at 96 Å clearly indicate that the experimental data are significantly higher than the prediction of the model assuming four screening electrons. The result of the C_5 cluster at 230 Å at this energy, see figure 4, corroborates this conclusion, as discussed above. It is not clear at this point why appreciably larger screening is required according to our model to fit the short penetration experimental data at the energy of 1 MeV/C. As has been noted above, this could be due to the approximations involved in assuming the potential in equation (1) or in the complexity of the cluster breakup process.

It is important to note that the results presented in figures 1–5 regarding the charge suppression do not depend on the absolute magnitude of the cross sections. Specifically, multiplying the ionization and recombination cross sections by a common factor essentially leaves the results unchanged.

Brunelle *et al* [3] raise the possibility that at the exit of the solid the vanishing of the screening effect would affect the charge state dynamics. Taking up on this point, the disappearance of screening, according to the model presented here, would enhance the bound electron binding energy, in accordance with equation (6), compared to that within the bulk solid.

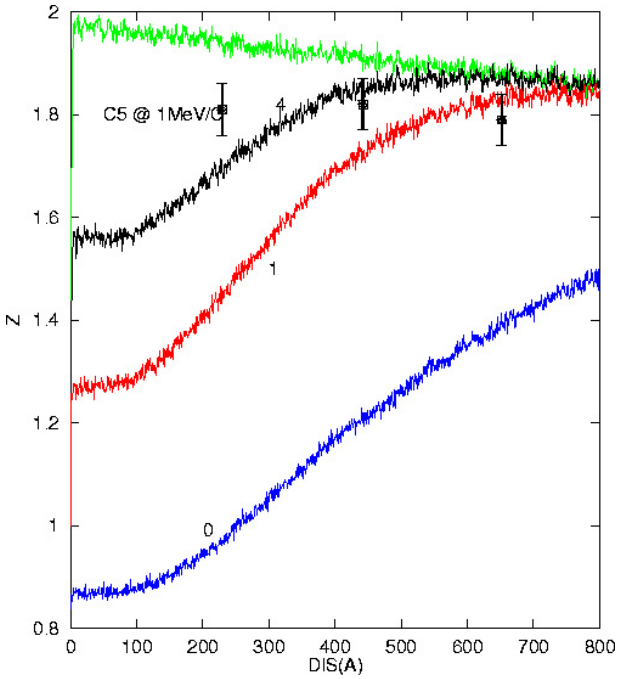

Figure 4. Average charge state of C_5 cluster at 1 MeV/C as a function of penetration depth, in ångströms, in an amorphous carbon target averaged over 500 different random sequences. Plotted separately are the calculated average charge states for the Coulomb interaction screened by four, one and no target valence electrons, with the number of screening electrons denoted adjacent to the appropriate plot. The experimental results [3] are presented at the three penetration depths. Also plotted is the calculated charge state for an individual carbon atom which is the top curve.

The ionization cross section would decrease while the recombination cross section increases, thus bringing about a further decrease in the charge state compared to the individual projectile. In order to test this we assumed the following simplified model and applied it to the C_{10} cluster at 2 MeV/C with four screening electrons: screening was abruptly turned off in a region defined between two planar parallel surfaces at the back of the target, where both surfaces were perpendicular to the initial cluster motion. The outer surface was the exiting surface at the back of the solid target, while the inner surface was assumed to be at a distance, a, the screening length, in the inward direction of the target. Results of the simulations show an insignificant change of the order of 1%–2% for various target thicknesses, resulting from the small value of a, in this case given by 1.5 Å.

In [5, 6] good agreement was obtained between their calculations and the experimental data for the 2 MeV/C experiments. Both these papers, however, do not treat the higher 4 and 1 MeV/C cluster beams, which we found to behave differently from the 2 MeV/C case. We also note once more that both these papers did not include scattering, while [6] also made no account of inter-ionic screening.

4. Discussion and conclusions

We have presented here detailed simulations of the interaction and breakup of energetic C_{10} and C_5 clusters at the energy of 2 MeV per carbon atom, at 4 MeV/C (only for C_5) as well as

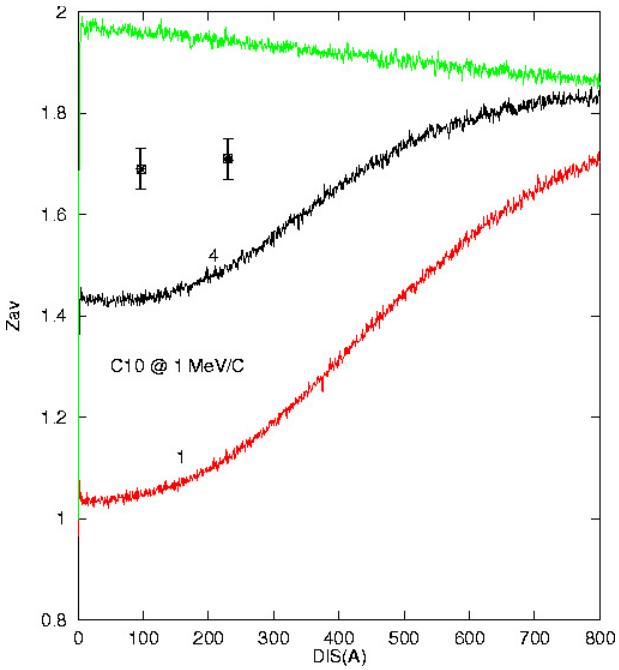

Figure 5. Average charge state of C_{10} cluster at 1 MeV/C as a function of penetration depth, in ångströms, in an amorphous carbon target averaged over 500 different random sequences. Plotted separately are the calculated average charge states for the Coulomb interaction screened by four and one valence electrons, with the number of screening electrons denoted adjacent to the appropriate plot. The experimental results [3] are presented at the two penetration depths. Also plotted is the calculated charge state for an individual carbon atom which is the top curve.

at 1 MeV/C, interacting with an amorphous carbon target. The calculations were performed using the algorithm described above, which is an extension of that of [1]. The improvement introduced here is in the treatment of the bound electron recombination, which is computed differently, using here the classical model of Bohr and Lindhard [4], which was used to calculate the influence of the other cluster ions on recombination. This was not calculated in [1], nor did [1] make specific comparisons to experimental data.

To summarize the results: good agreement between the calculated and experimental charge state is obtained up to the penetration distance of 443 Å, with the assumption of four screening electrons for the 2 MeV/C C_{10} clusters, while for C_5, since no experimental point is available at 443 Å, we could only state that agreement is good up to 230 Å. However, with increasing penetration, fewer screening electrons are needed to fit the experimental data, in particular at 1739 Å, where it is doubtful that the present model is still valid, but also at 650 Å for both C_{10} and C_5.

It is reasonable that the model here should not be able reproduce the experimental results at large penetration distances, where the inter-particle distances are relatively large. The simple spherical symmetrical Yukawa potential adopted here is but an approximation to the correct dynamical screening potential. The screening length a in figures 1 and 2 is 1.5 Å, while the average interparticle distance for C_{10} at 650 Å is 5.58 Å, becoming larger with increasing depth of penetration. The distances involved here for the 650 Å case are thus of the order of almost four times the exponential attenuation distance. The correct potential probably does not follow the exponential decay up to this relatively large distance, and the potential calculated using

the present model for 650 Å probably decays too rapidly and is therefore too small. Thus, in order to compensate for this, fewer screening electrons are required, the effect of which is to increase the intra-cluster potential. Thus we cannot attribute physical meaning to the one and zero screening electrons obtained at the larger depths within the framework of the present model.

For the C_5 higher energy 4 MeV/C cluster, the results of our model in comparison with experiment show the same trend as for the 2 MeV/C clusters; however, less screening in comparison to the 2 MeV/C cases is needed to fit the experimental data. A possible and plausible explanation as noted above is the inability of the plasma to completely shield the faster moving projectile. In comparing the lower energy, 1 MeV/C, C_5 and C_{10} clusters with our model, a behaviour different from the 2 and 4 MeV/C clusters is obtained. The experimental points at penetration depths less than 230 Å are significantly higher than the prediction of the model assuming four screening electrons, and the trend of the experimental points as a function of penetration depth is different from that of the calculation and different from the behaviour of the higher energy clusters. At these relatively low projectile kinetic energies we cannot suggest an excitation mechanism whereby more than four electrons dynamically screen the projectile and no explanation is apparent for the different behaviour between the 2 and 1 MeV/C clusters.

In the context of the experimental results for the 2 MeV/C clusters we discuss other experimental evidence on the effective number of valence electrons in amorphous carbon. We cite the resonance in the measured stopping power of 30 keV electrons in carbon, which gives $h\omega_p = 25.9$ eV [30], and the measured stopping power of 400 keV protons (equivalent to 4.8 MeV carbons), which gives $h\omega_p = 25$ eV [31]. The associated value of the number of active valence electrons in these targets is inferred to be 4.5. Analyses of the effective number of valence electrons, N_{eff}, as a function of plasmon excitation frequency is given by Abril *et al* [32] for amorphous carbon, based on dielectric theory. N_{eff} was found to be of the order of four for a wide range of excitation energies in the region from about 1 to 10 au, with the core electrons coming into play only at much higher excitation energies. Taft and Phillips [33] studied the optical properties of graphite in detail, on the basis of which they derive the energy loss function. These authors find a strong resonance at 25 eV associated with plasma oscillations involving the combined π and σ electrons, which together constitute four electrons per atom. Our analysis of the charge suppression experimental data employing the Bohr and Lindhard model [4], for the 2 MeV/C recombination model, indicates that the Coulomb interaction within the amorphous carbon target is screened by four valence electrons a result which is close to other experimental data regarding the number of effective valence electrons.

The physics of cluster–solid interaction is such a complex issue, however, that one cannot rule out the possible influences of various other aspects of the interaction not accounted for in our model. Still, it could be argued that the main result of the study is that it shows quite reasonable general agreement for most of the cases studied at penetration depths up to 450 Å, and the physics of the phenomena is fairly well represented by the assumptions of the model, with the exception of the 1 MeV/C data. That the results of the present simulations do not perfectly agree with experiment is acceptable, since the problem at hand is a very complex one.

We note that the very recent experimental results of Chiba *et al* [34] essentially confirm those of Brunelle *et al* [3] for the C5 cluster at 1 MeV/C. These authors, however, do not provide experimental information on the 2 and 4 MeV/C cases. Any additional experimental data, different kinetic energies or other energetic clusters, would be of very great interest for the analysis of the cluster breakup phenomenon using the tools of the present work.

In future work the use of a more realistic potential could be considered, perhaps based on the dynamically screened Coulomb interaction derived by means of the linear-response

dielectric theory, similar to the calculation of Wei *et al* [7]. It is our opinion that the results of the present study also call for further experimentation, specifically, measuring charge suppression for additional cluster energy and cluster size combinations. Replacing the carbon foil target by other solid material could be of significant interest. In particular, one could consider using metallic or dielectric targets and analysing the results within the framework of the present model. The latter target is of special interest since analysis of the type carried out here could ascertain how many valence electrons, in the otherwise inert target, are excited by the incoming energetic fragments and partake in the screening of the Coulomb potential.

Acknowledgments

This work was partially supported by the German–Israeli Project Cooperation Foundation (DIP) and the Israel Science Foundation. The authors would also like Professor N Arista for his valuable comments.

References

[1] Nardi E, Zinamon Z, Tombrello T A and Tanushev N M 2002 *Phys. Rev.* A **66** 013201
[2] Hartman J W, Tombrello T A, Bouneau S, Della-Negra S, Jacquet D, Le Beyec Y and Pautrat M 2000 *Phys. Rev.* A **62** 043202
[3] Brunelle A, Della Negra S, Depauw J, Jacquet D, Le Beyec Y and Pautrat M 1999 *Phys. Rev.* A **59** 4456
[4] Bohr N and Lindhard J 1954 *K. Dan. Vidensk. Selsk. Mat.-Fys. Medd.* **28** (7)
[5] Heredia-Avalos S, Garcia-Molina R and Arista N R 2001 *Europhys. Lett.* **54** 729
[6] Kaneko T 2002 *Phys. Rev.* A **66** 052901
[7] Wei H-W, Wang Y-N and Miskovic Z I 2004 *J. Phys.: Condens. Matter* **16** 1231
[8] Moller W, Popiech G and Schrieder G 1975 *Nucl. Instrum. Methods* **130** 265
[9] Zaijfman D, Graber T, Kanter E P and Vager Z 1992 *Phys. Rev.* A **46** 194
[10] Barriga-Carrasco M D and Garcia-Molina R 2004 *Phys. Rev.* A **70** 032901
[11] Gemmell D S, Remillieux J, Poizat J-C, Gaillard M J, Holland R E and Vager Z 1975 *Phys. Rev. Lett.* **34** 1420
[12] Richard P 1985 *Atomic Inner Shell Processes I* ed B Crassman (New York: Academic) p 73
[13] McGuire J H and Richard P 1973 *Phys. Rev.* A **3** 1374
[14] Gryzinski M 1965 *Phys. Rev.* **138** A336
[15] Schiwietz G, Schneider D and Tanis J 1987 *Phys. Rev. Lett.* **59** 1561
[16] Andersen J U, Gruner F, Ryabov V A and Uguzzoni A 2002 *Nucl. Instrum. Methods* B **193** 118
[17] Betz H D 1983 *Applied Atomic Collision Physics* vol 4, ed S Datz (New York: Academic) p 1
[18] Eichler J and Chan F T 1979 *Phys. Rev.* A **20** 104
[19] Sols E and Flores F 1988 *Phys. Rev.* A **37** 1469
[20] Stoller Ch *et al* 1983 *IEEE Trans. Nucl. Sci.* **30** 1074
[21] Lifschitz A F and Arista N R 2004 *Phys. Rev.* A **69** 012902
[22] Brandt W 1975 *Atomic Collisions in Solids* ed S Datz, B R Appelton and C D Moak (New York: Plenum) p 261
[23] Lindhard J 1954 *K. Dan. Vidensk. Selsk. Mat.-Fys. Medd.* **28** (8)
[24] Nagy I and Bergara A 1996 *Nucl. Instrum. Methods* B **115** 58
[25] Lifschitz A F and Arista N R 1998 *Phys. Rev.* A **57** 200
[26] Jakubassa D H 1977 *J. Phys. C: Solid State Phys.* **10** 4491
[27] Chevallier M, Clouvas A, de Castro Faria N V, Farizon Mazuy B, Gaillard M J, Poizat J C, Remillieux J and Désesquelles J 1990 *Phys. Rev.* A **41** 1738
[28] Bouyer R 1995 *PhD Thesis* Universite Paris IX Orsay (unpublished)
[29] Nicholson D R 1983 *Introduction to Plasma Theory* (New York: Wiley) p 219
[30] Burge R E and Mosell D L 1983 *Phil. Mag.* **18** 251
[31] Vager Z and Gemmell D S 1976 *Phys. Rev. Lett.* **34** 1420
[32] Abril I *et al* 1998 *Phys. Rev.* A **58** 357
[33] Taft E A and Philipp H R 1965 *Phys. Rev.* A **138** 197
[34] Chiba A, Saitoh Y and Tajima S 2005 *Nucl. Instrum. Methods* B **232** 32